

**Note to readers with disabilities:** *EHP* strives to ensure that all journal content is accessible to all readers. However, some figures and Supplemental Material published in *EHP* articles may not conform to [508 standards](#) due to the complexity of the information being presented. If you need assistance accessing journal content, please contact [ehponline@niehs.nih.gov](mailto:ehponline@niehs.nih.gov). Our staff will work with you to assess and meet your accessibility needs within 3 working days.

## **Supplemental Material**

### **Expansion of the Lyme Disease Vector *Ixodes scapularis* in Canada Inferred from CMIP5 Climate Projections.**

Michelle McPherson, Almudena García-García, Francisco José Cuesta-Valero, Hugo Beltrami,  
Patti Hansen-Ketchum, Donna MacDougall, and Nicholas Hume Ogden

#### **Table of Contents**

**Figure S1.** Annual estimates of the  $R_0$  multi-model mean, the model variability (95% confidence interval) and the estimated numbers of Census Subdivisions (CSDs) with established *I. scapularis* populations for Nova Scotia.

**Figure S2.** Annual estimates of the  $R_0$  multi-model mean, the model variability (95% confidence interval) and the estimated numbers of Census Subdivisions (CSDs) with established *I. scapularis* populations for Ontario south of 50°N.

**Figure S3.** Multi-model mean  $R_0$  values for *I. scapularis* and the climate model variability using RCP2.6 simulations.

**Figure S4.** Multi-model mean  $R_0$  values for *I. scapularis* and the climate model variability using RCP6.0 simulations.

**Figure S5.** The spatial differences between  $R_0$  multi-model mean estimates of each successive RCP scenario for the time periods 2011-2040 and 2041-2070.

**Figure S6.** Annual estimates of the  $DD > 0^\circ\text{C}$  multi-model mean values under the RCP6.0 and RCP4.5 scenarios.

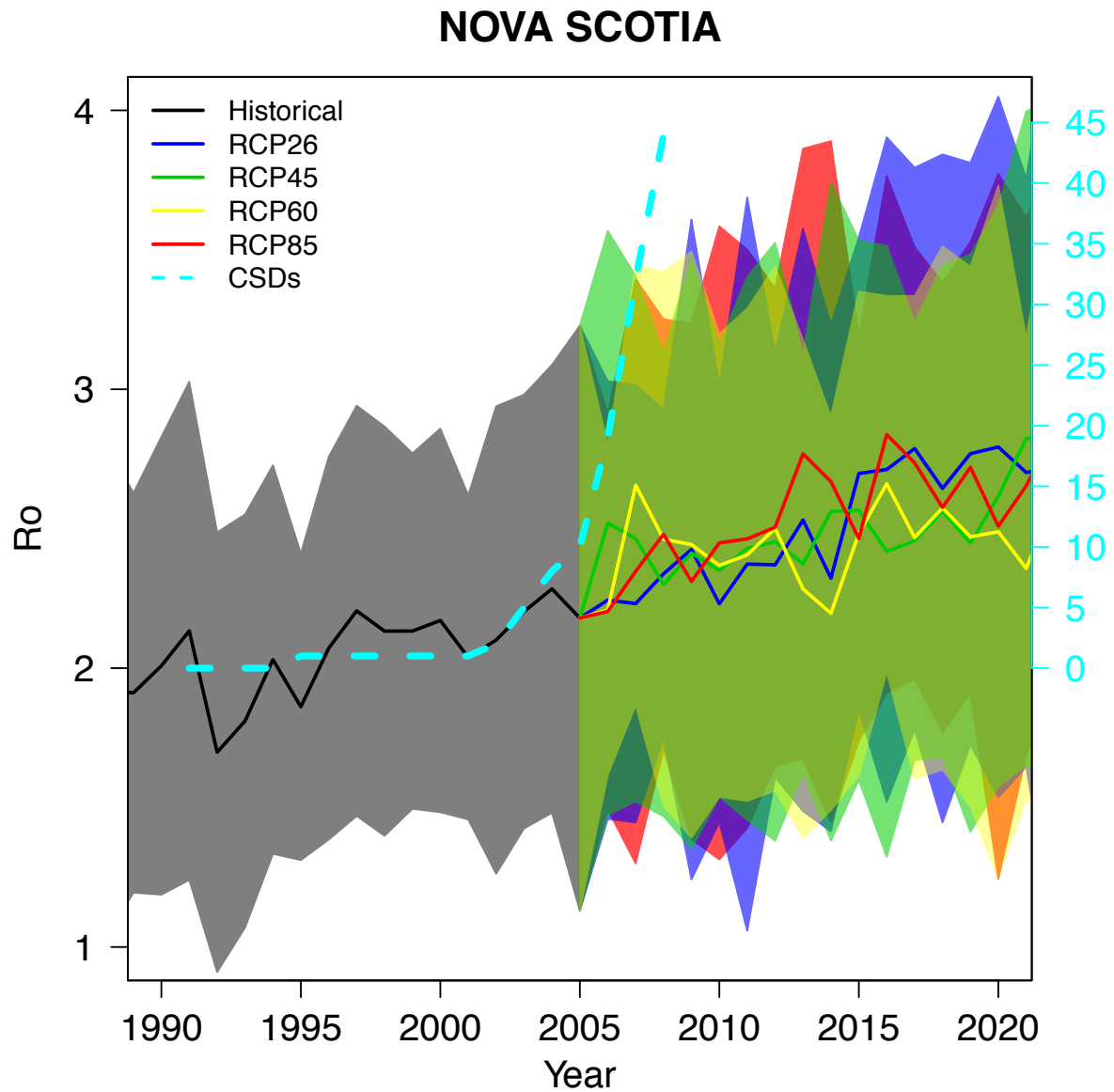


**Figure S1.** Annual estimates of the  $R_0$  multi-model mean and the model variability (95% confidence interval) for Nova Scotia from 1985 to 2025. The estimated numbers of Census Subdivisions (CSDs) with established *I. scapularis* populations in Atlantic Canada, based on passive surveillance data (Leighton et al. 2012), is shown as the light-blue dashed line.

## SOUTHERN ONTARIO

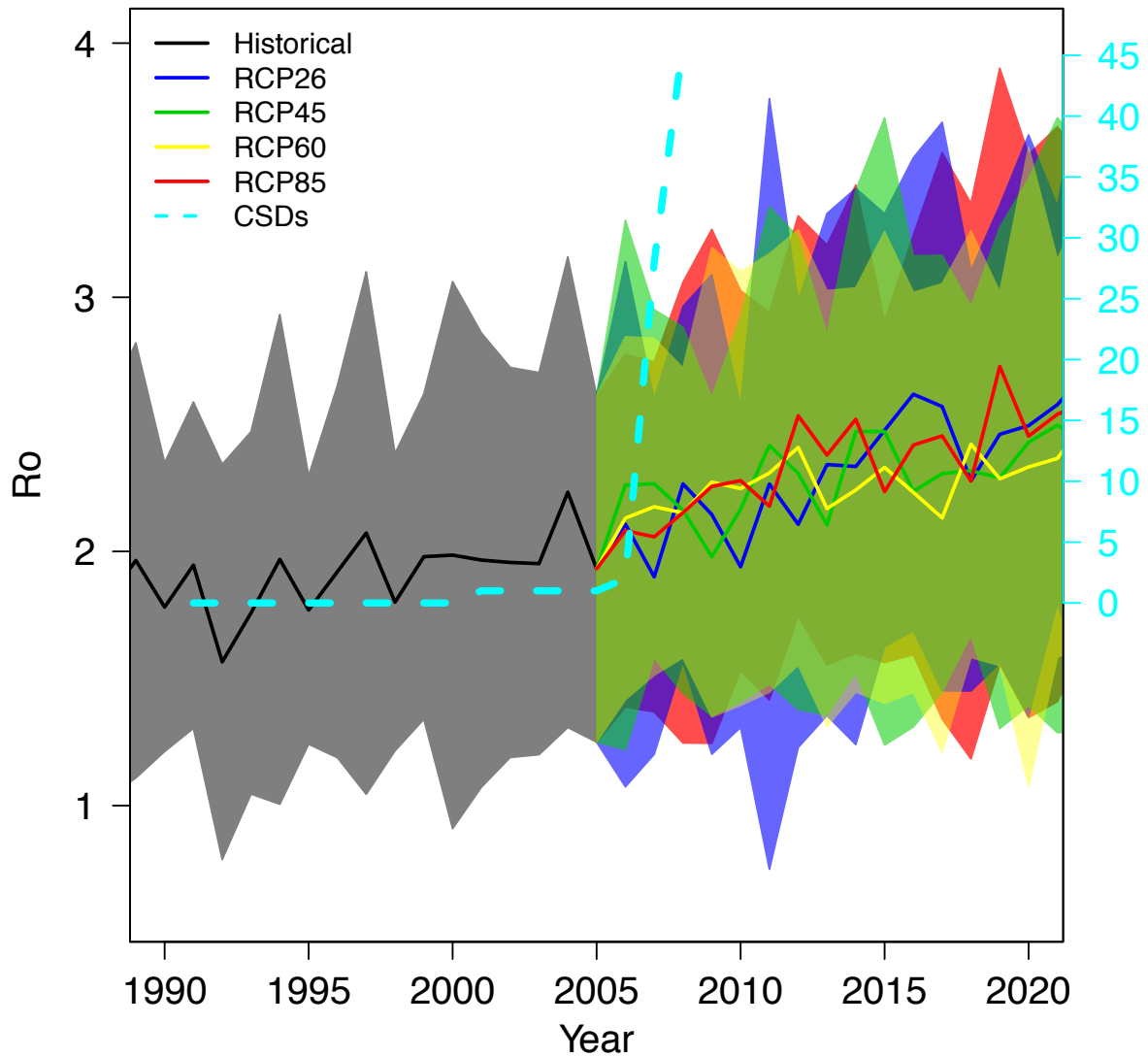


**Figure S2.** Annual estimates of the  $R_0$  multi-model mean and the climate model variability (95% confidence interval) for Ontario south of 50°N from 1985 to 2025. The estimated numbers of Census Subdivisions (CSDs) with established *I. scapularis* populations in Ontario, based on passive surveillance data (Leighton et al. 2012), is shown as the light-blue dashed line.

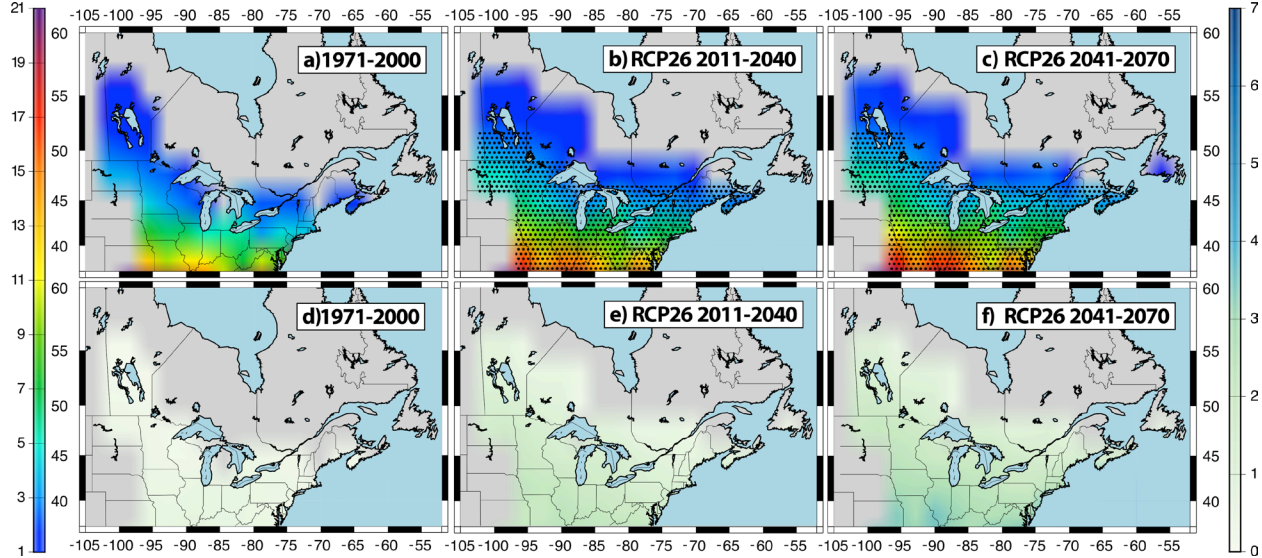


**Figure S3.** Multi-model mean  $R_0$  values for *I. scapularis* (maps a-c) and the climate model variability (95% confidence interval) (maps d-f) for the period 1971 to 2000 using the historical simulations and for the periods 2011 to 2040 and 2041 to 2070 using RCP2.6 simulations.  $R_0 > 1$  values were mapped for areas east of the Rocky Mountains and for elevations below 500m. The  $R_0$  bar provides a color gradient showing the colors, which correspond to specific  $R_0$  values. The numbers around the maps depict the northings and eastings associated with the domain. Black stippling in maps b and c shows the spatial distribution of statistically significant changes in  $R_0$  between each future time period, 2011-2040 and 2041-2070, and the historical time period, 1971-2000. Statistical significance was calculated using the Kolmogorov-Smirnov test at the 95% confidence level.

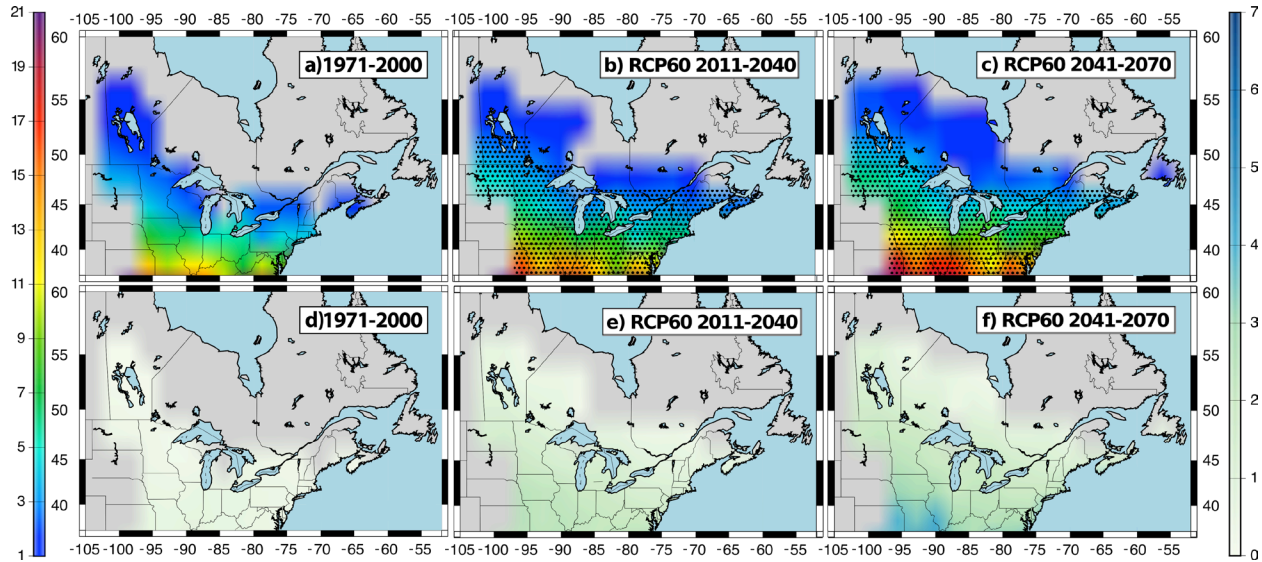


**Figure S4.** Multi-model mean  $R_0$  values for *I. scapularis* (maps a-c) and the climate model variability (95% confidence interval) (maps d-f) for the period 1971 to 2000 using the historical simulations and for the periods 2011 to 2040 and 2041 to 2070 using RCP6.0 simulations.  $R_0 > 1$  values were mapped for areas east of the Rocky Mountains and for elevations below 500m. The  $R_0$  bar provides a color gradient showing the colors, which correspond to specific  $R_0$  values. The numbers around the maps depict the northings and eastings associated with the domain. Black stippling in maps b and c show the spatial distribution of statistically significant changes in  $R_0$  between each future time period, 2011-2040 and 2041-2070, and the historical time period, 1971-2000. Statistical significance was calculated using the Kolmogorov-Smirnov test at the 95% confidence level.

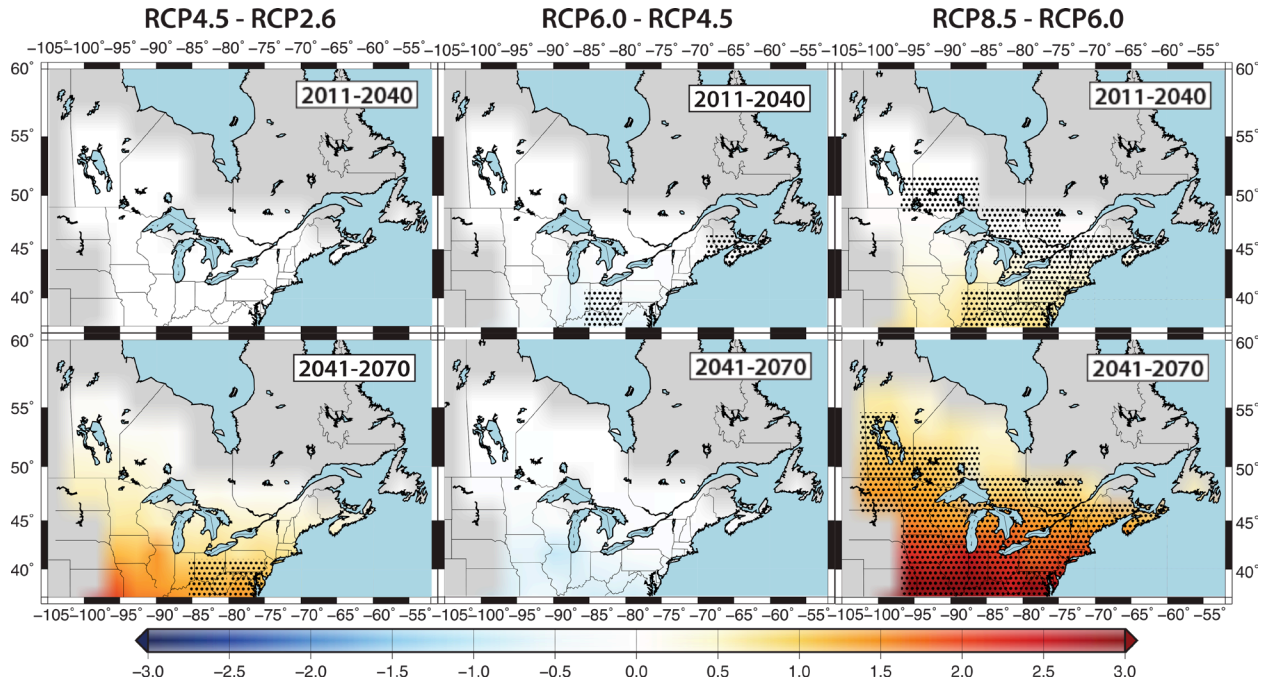


**Figure S5.** The spatial differences between  $R_0$  multi-model mean estimates of each successive RCP scenario for the time periods 2011-2040 (top row) and 2041-2070 (bottom row). The color bar indicates differences, in terms of  $R_0$  multi-model mean values – that exist between successive RCPs; darker red areas indicate large positive difference between successive RCP scenarios, darker blue indicates large negative differences between successive RCP scenarios. The numbers around the maps depict the northings and eastings associated with the domain. The black stipples show the spatial distribution of statistically significant differences between the  $R_0$  multi-model mean estimates under each successive RCP. Statistical significance was calculated using the Kolmogorov-Smirnov test at the 95% confidence level.

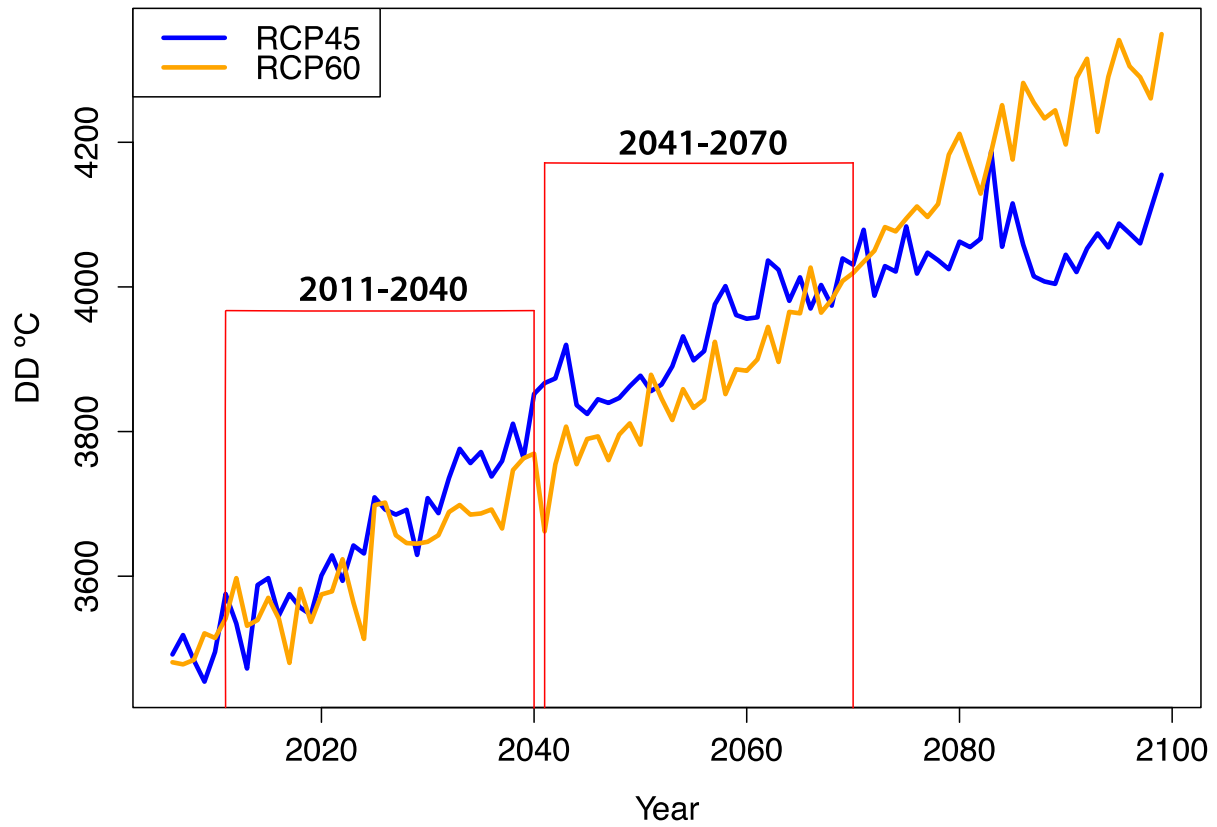


**Figure S6.** Annual estimates of the  $DD > 0^{\circ}\text{C}$  multi-model mean values under the RCP6.0 and RCP4.5 scenarios for our domain, taking into account the elevation limit of 500m. The red lines mark the time periods in which multi-model mean  $R_0$  values for *I. scapularis* and the associated climate model variability were mapped.